Journal of Inclusion Phenomena and Macrocyclic Chemistry (2006) 56: 161–166
DOI 10.1007/s10847-006-9077-2

Confinement Effects of Cyclodextrin on the Photodynamics of Few Selected Systems

J.A. ORGANERO, L. TORMO, M. SANZ, L. SANTOS and A. DOUHAL*
Departamento de Química Física, Sección de Químicas, Facultad de Ciencias del Medio AmbienteUniversidad de Castilla-La Mancha, Avda. Carlos III, S.N. 45071, Toledo, Spain

Key words: absorption, anisotropy, confinement, cyclodextrins, emission

Abstract

In this contribution, we discuss the effect of cyclodextrins (CDs) on the photorelaxation of three molecules showing proton and charge transfer reactions. Using steady-state and picosecond time-resolved emission spectroscopy, we show that the confinement due to the restriction of CDs and the H-bonding network of their OH-groups involving water molecules found at its gates play an important role for both spectral and time domains. Anisotropy experiments give different rotational times following the nature and stoichiometry of the formed complexes.

Introduction

Cyclodextrins (CDs) have been revealed as effective nanosystems to encapsulate different molecules. Their caging ability modifies the degrees of freedom of the reaction coordinates of the guests following the characteristic of the CDs. For example, the dynamics of elemental processes in chemistry like that of breaking and making chemical bonds, proton and charge transfer, twisting motion and salvation can be changed by caging the related aromatic guest [1–14]. In this article review, we focus on the results of studying three molecules (Scheme 1) in solution and in CDs: methyl 2-amino-4,5-dimethoxy benzoate (ADMB), 3-hydroxyflavone (3HF) and 1′-hydroxy-2′-acetonaphthone (HAN). These systems, studied in this laboratory, show a high sensitivity to the nature of the environments.

ADBM is an anesthetic analogous to procaine and tetracaine with two groups able to form an intramolecular H-bond [13, 15]. This bond is comparable to that found in methyl salicylate, where the hydroxyl group has been substituted by the amino one. The binding phenomena with CD might be considered as a model to mimic the interactions of drugs with hydrophobic pockets of CDs and biological substrates.

3HF is a widely studied molecule that undergoes an excited-state intramolecular proton-transfer (ESIPT) reaction from its first excited electronic state (S_1) to give a zwitterionic tautomer (Z) [16–19]. In hydrogen bonding media, H-bonded structures to the solvent molecules give normal emission at blue side, and detection of anionic forms at the S_0 and S_1 states has been reported [20–23]. In cyclodextrins, the H-bonding networks of CDs play an important role in the stabilization of anionic structure [12].

HAN is an aromatic molecule that undergoes an ESIPT reaction, within 30 fs [24], and a subsequent twisting motion of the protonated acetyl group of the formed keto (K*) tautomers giving birth to a keto rotamer (KR*) at the S_1 state. This results have been predicted by theoretical calculations and experimentally observed in gas, liquids and in CD solutions [10, 11, 24–28].

In this article review, we will show the effects of the caging interactions and the environments of the cyclodextrins on the photodynamic of these molecules. Details can be found in the original contributions [10–13].

Experimental

ADMB was synthesized by a simple esterification procedure of its acid derivative (Sigma-Aldrich). The purity of the sample was checked by ^{1}H NMR, IR, elemental analysis, and thin-layer chromatography. HAN, 3HF, CDs (from Sigma-Aldrich) and all the solvents (spectrograde quality) were used as received. Their purity was checked before use except anhydrous N,N-dimethylformamide (DMF, Sigma-Aldrich, 99.8%) that was used after drying and purification by standard methods. Details on the apparatus and procedures of getting the data and their analysis were described [10–13].

Results and discussion

Methyl 2-amino-4,5-dimethoxy benzoate (ADMB)

At the S_0 state, ADMB presents an $NH_2\cdots O=C–O$ intramolecular H-bond in organic solvents (Scheme)

* Author for Correspondence. E-mail: abderrazzak.douhal@uclm.es

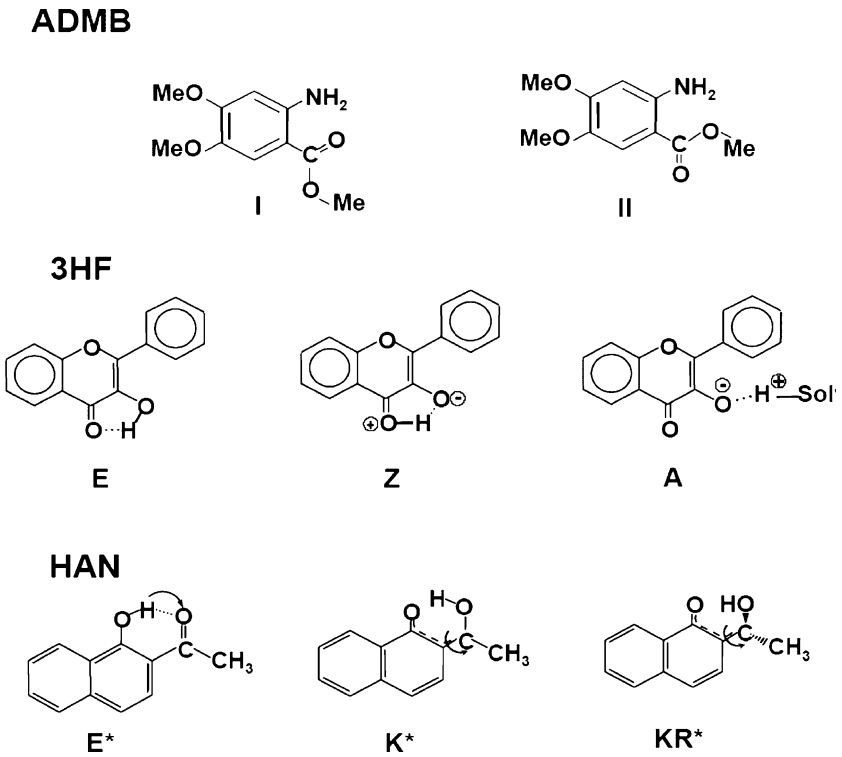

Scheme 1. Molecular structures of the studied guests.

which becomes stronger at S_1. The position of the maxima in absorption spectra depends on the polarity and H-bonding properties of the solvent [15]. In neutral water, the lowest absorption band ($S_0 \rightarrow S_1$) has the maximum at 340 nm. Upon addition of β-CD, the absorption spectrum remains unchanged. Upon excitation at 340 nm, the emission spectrum (Figure 1) shows an increase in the emission band intensity which shows a large Stokes shifts ($\sim$7400 cm^{-1}) [13]. This is explained in terms of an intramolecular charge-transfer (ICT) reaction from the amino group to the phenyl part, and not due to an ESIPT as it occurs in the analogous molecule antharanilic acid [29, 30]. Thus, the increase in the emission intensity upon addition of β-CD is not a consequence of the formed phototautomers, but as a result of an enhanced emission of the caged intramolecular H-bonded ADMB molecule within β-CD. Analyzing the variation of emission intensity with [β-CD], we determined that the stoichiometry of the formed complex is 1:1, and the equilibrium constant value associated to this process at 293 K is 12 ± 3 M^{-1}.

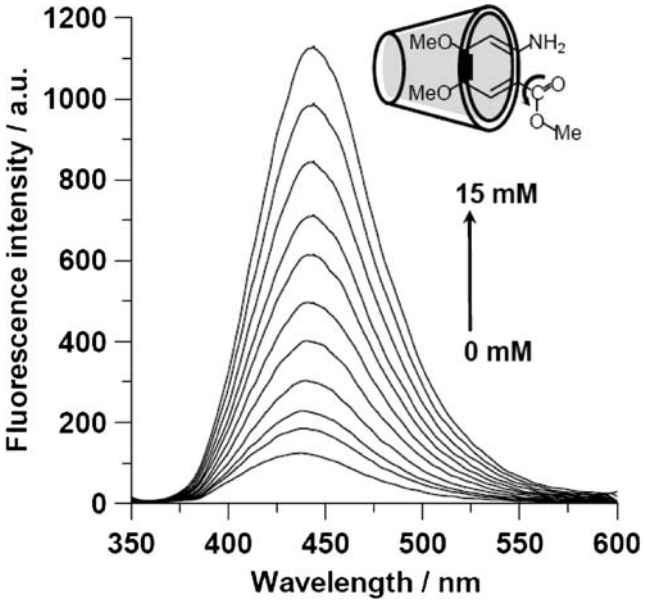

Figure 1. Change in the emission spectrum of ADMB in water upon addition of β-CD. Excitation at 340 nm, and $T = 293$ K. The inset shows the confined structure of ADMB with CD.

Using the mean value of the emission lifetime of the complexes (2.9 ns) and the calculated radiative lifetime (10 ns), we obtained the emission quantum yield of the complexes, $\phi = 0.29$. This value is quite large compared to that obtained in pure water, $\phi = 5 \times 10^{-3}$. This indicates the presence of efficient non-radiative processes in water. These might be due to intermolecular H-bonding interactions with the solvent or twisting motion of the amino groups of the dye. Furthermore, we observed a strong dependence of the fluorescence lifetimes on the viscosity and H-bonding character of the solvent. Thus in methanol, we obtained a bi-exponential decay with 0.9 ns (70%) and 2.2 ns (30%). While in 1-decanol, these times are 1.8 (10%) and 6.3 ns (90%). The dependence of the lifetimes on the viscosity and polarity of the alcohols is a consequence of the involvement conformational changes due to twisted configurations of ADBM (Scheme). The efficiency of these non-radiative channels is reduced due to the confinement effects on the ADBM into β-CD.

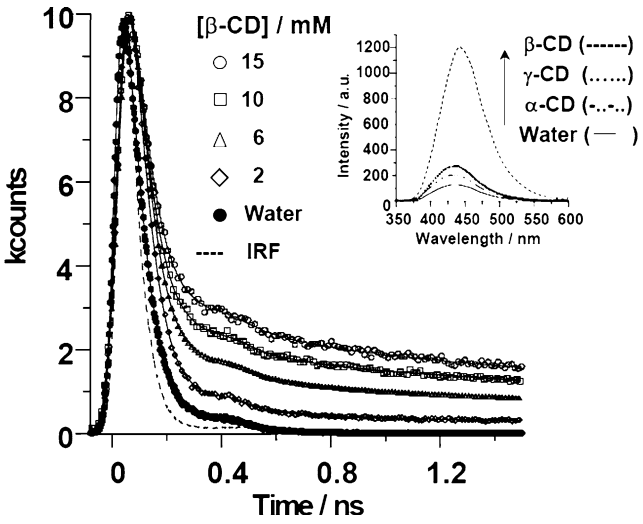

Figure 2. Magic-angle fluorescence decays of ADMB in neutral water and in presence of β-CD. Excitation was done at 371 nm and emission was gated at 480 nm. The instrumental response function (IRF) is ~65 ps. The Inset shows emission spectra of ADMB in neutral water and in presence of 15 mM, α-, β-, γ-CD, upon excitation at 340 nm.

To get information on the picosecond dynamics of the formed complexes in β-CD, we measured the emission decays of ADBM in water and in presence of β-CD (Figure 2). In neutral water, the emission decay at 450 nm fits to a bi-exponential function with time constants of 47 ± 10 ps (93%) and 110 ± 15 ps (7%). The assignment of these times was based on theoretical calculations (B3LYP/6-31G**) that predict that conformer I is only 1.84 kcal/mol more stable than II, and the dipole moments are 1.53 and 4.89 D, respectively. Therefore it is expected that in water solution, conformer II (with a larger dipole moment) will be more stable than I. In addition to that, the calculations predict that the internal H-bond in II is 0.039 Å, shorter than in I. Therefore non-radiative processes due to twisting motion are expected to be faster in II than in I, leading to shorter emission lifetime for II when compared to I.

In presence of β-CD, a four-exponential function was needed to obtain an accurate fit (Figure 2). For example at [β-CD] = 15 mM and gating the emission at 450 nm, the obtained lifetimes are: 40 ps (67%), 110 ps (22%), 0.8 ns (3%) and 3.7 ns (8%). The ps-components are assigned to free II and I conformers, respectively. The amplitude of the 110 ps component increases with [β-CD]. This is explained in terms of complexing conformer II rather than conformer I. The two other ns-components, whose pre-exponential factors increase with the [β-CD] are due to ADMB:CD complexes. The confinement effects on the photodynamic of the molecule leads to larger lifetimes of the trapped ADMB. It is worth to note that depending on the gated emission wavelength, the ns-component varies between 0.6–1.1 and 3.4–3.9 ns, respectively. For the first one, there is no change in its amplitude. However, it increases at longer wavelengths of observation for the second one. This behavior is explained in terms of a heterogeneous environment of the complexes having different conformations of the guest and different interactions with water molecules. Thus, the longest ns-component corresponds to more protected complex than the shortest one. This later is more exposed to water interactions that break the intramolecular H-bond and therefore favors the twisting of the ester group like in the II conformer. The observed caging effects in a smaller nanocavity (α-CD) and in a larger one (γ-CD) are not so significant in steady-state (Inset Figure 2) and in time-resolved measurements. In the case of the complex with α-CD, the ADMB molecule does not penetrate enough into the cavity. The amino and ester groups are still exposed to water molecules. For the case of the complex with γ-CD, the twisting motion is highly favored due to a larger cavity giving faster decays.

For time-resolved anisotropy measurements of ADMB in β-CD solution (15 mM), the decays give two rotational times $\phi_1 = 53 \pm 20$ ps (40%) and $\phi_2 = 510 \pm 50$ ps (60%). ϕ_1 is assigned to the rotational relaxation of the caged guest. This component also contains a contribution of the rotational time of free ADMB, as measured in pure water (~97 ps), while ϕ_2 is assigned to an overall rotational time of the confined complex of ADMB:β-CD which is close to 520 ps obtained using the Debye–Stokes–Einstein hydrodynamic theory under stick conditions.

3-hydroxyflavone

The steady-state measurements of 3HF in DMF and in presence of γ-CD are shown in Figure 3. The UV-visible absorption spectrum shows at ~425 nm the formation of the anion (A) of 3HF. Adding γ-CD produces an increase in the anionic absorption band intensity, and a decrease in the enol (E) one at ~340 nm (Figure 3a). Addition of 1.5 M of water does not significantly change the spectrum. A similar behaviour was observed upon addition of maltose (two linked glucose units with eight OH groups). These phenomena are explained in terms of formation of an anionic inclusion complex of 3HF into γ-CD whereas the OH group of the caged 3HF has been deprotonated increasing its acidity with the H-bonding network formed by the OH groups of γ-CD.

In the case of complexation with β-CD (CD with a smaller internal diameter than γ-CD), the increase in the absorption intensity of the anionic band is very weak (5–10%) upon addition of 120 mM of β-CD. The observed changes in absorption spectra were analyzed assuming the formation of an 1:1 inclusion complex between 3HF and CD. The obtained equilibrium constants are 48 M^{-1} and 0.2 M^{-1} at 293 K, respectively, indicating a larger stabilization into γ-CD than in β-CD. The stabilization is due to hydrophobic effect and H-bonding interactions with CD pocket.

The emission spectra (Figure 3b) of these solutions when exciting at 420 nm show an increase in intensity upon addition of CD due to the formation of a more fluorescent molecule as consequence of confinement effects on the caged anion. When exciting at 320 nm

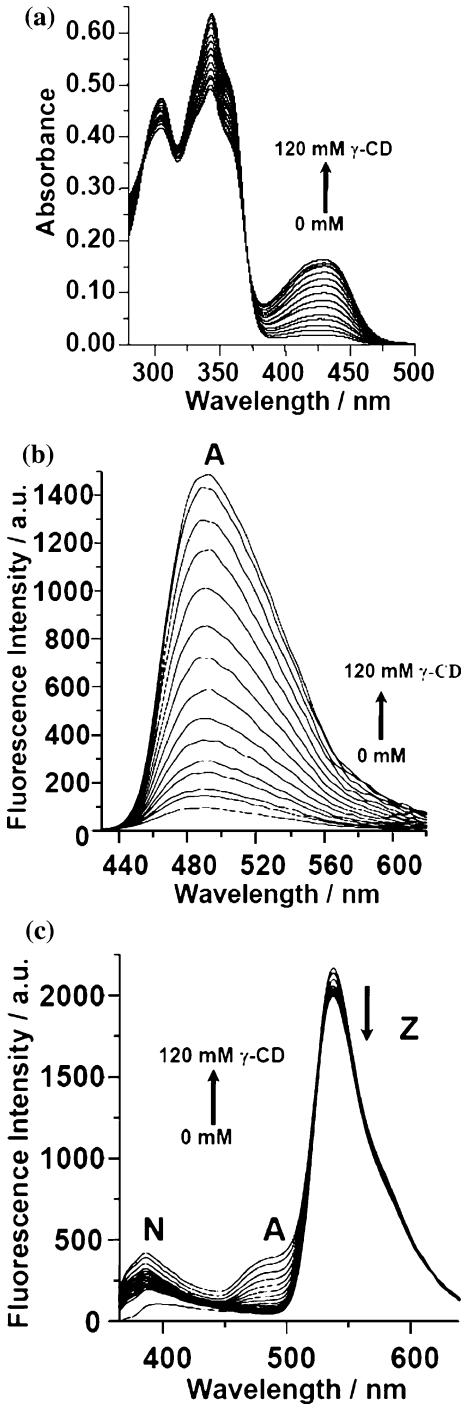

Figure 3. (a) UV-visible absorption and (b, c) emission spectra of 3HF in N,N-dimethylformamide upon addition of different concentrations of γ-CD. For (b) and (c) the excitation wavelengths were 420 and 340 nm, respectively. E, A and Z within the figure indicates the emission bands corresponding to enol, anion and zwitterionic species, respectively.

(Figure 3c), we observed three emission bands at 380, 480 and 520 nm assigned to 3HF bonded molecules to γ-CD (more fluorescence than those bonded to DMF), anion (A) and zwitterions (Z) structures, respectively. The excitation spectrum of 3HF (not shown) in a saturated solution of γ-CD reveals a $\sim$15 nm red-shift compared to that collected in pure DMF. This is due to a larger relaxation of the guest inside this pocket, allowing a larger electronic conjugation between the aromatic frames of anionic 3HF.

From the point of view of relaxation to the ground state, the emission decay of 3HF in pure DMF at 480 nm fits to a three-exponential function with time constants of $\sim$10 ps (99%), $\sim$273 ps (0.7%) and $\sim$1.9 ns (0.3%) assigned to E, Z and A conformers, respectively. Upon addition of 120 mM of γ-CD, these values change to $\sim$12 ps (68%), $\sim$270 ps (7%) and $\sim$2.14 ns (25%). The increasing on the population of the ns component is because the caged A is more excited at this wavelength. Gating the decay at 560 nm, a 12-ps rising component was observed close to the one assigned to the proton transfer motion to produce Z, according to the obtained value in [23].

The observed rotational times obtained from the time resolved anisotropy experiments reveal also the formation and characteristics of the formed complexes. In pure DMF, we obtained a single exponential decay with rotational time, $\phi = \sim$85 ps. Upon addition of CD we obtained two-exponential decays with rotational times $\phi_1 = \sim$169 ps, $\phi_2 = \sim$474 ps for 3HF:γ-CD complexes, and $\phi_1 = \sim$175 ps, $\phi_2 = \sim$438 ps for 3HF:β-CD ones. In both cases ϕ_1 is twice that of free 3HF in DMF indicating a docking of A into the cavity while ϕ_2 corresponds to the overall rotational time of the complexes.

1′-hydroxy-2′-acetonaphthone (HAN)

HAN is a prototype system showing a photo-induced intramolecular proton-transfer reaction to give a keto (K*) tautomer followed by a twisting motion to produce a more stable keto tautomer (KR*). In this section, we will shortly review the results of the nanocavity studies of HAN with α- β- and γ-CD.

The binding constants and stoichiometry of the inclusion complexes of HAN with CD's were deduced using the change in the emission intensity [10, 11]. We found that for HAN:β-CD and HAN:γ-CD, the formed complexes have an 1:1 stoichiometry. The equilibrium constant values at 300 K are 1385 ± 150 M^{-1} and 910 ± 120 M^{-1}, respectively. For HAN:α-CD, we found 1:1 and 1:2 stoichiometries with equilibrium constants: $K_{1:1} = 2 \pm 1$ M^{-1} and $K_{1:2} = 273 \pm 100$ M^{-1} at 300 K.

Figure 4a shows the emission spectra gated at 1 ns of HAN in α-, β-, γ-CD solutions. For a larger cavity (γ-CD), the emission band of HAN:γ-CD shifts to the red (maxima at 500 nm) when compared to HAN:β-CD and HAN:α-CD emission (maxima at 460 nm). This spectral shift is due to a larger protection (from H-bonding interactions with water) and relaxation of the photo-tautomers into the γ-CD. The photodynamic relaxation involves rotational motion of $COHCH_3$ group. In a smaller cavity, the rotation of this group is restricted allowing a larger population of a keto-type tautomer (K*) that emits at the blue part of the spectrum. Clearly this spectral change is related to the time domain. Thus, we recorded the emission decays of HAN in water and

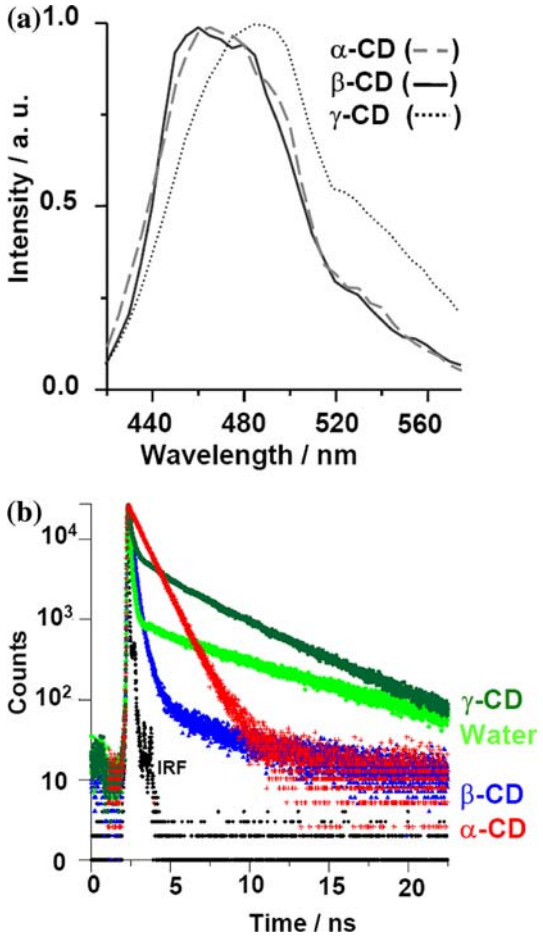

Figure 4. (a) Emission spectra of HAN in presence of $\sim 10^{-3}$ M of α-, β-, and γ-CD gated at 1 ns. (b) Emission decays at 480 nm (magic angle) of HAN in water and in CD solutions upon excitation at 393 nm. See text for the values of time constant of the decaying signal. IRF is the instrument response function.

in saturated solutions of CD's (Figure 4b). In neutral water, the emission decay fits to a bi-exponential function giving time constant of ~90 ps (99%) and 5–6 ns (1%), assigned to free K* and KR* tautomers, respectively. Upon addition of 15 mM of β-CD, the lifetime values are ~90 ps (34%), ~200 ps (63%), and ~742 ps (3%). The first ps-component has the same origin as in pure water, while the two other components are assigned to the encapsulated tautomers K* and KR*, respectively. These lifetimes are shorter than those observed in water because the twisting of HAN in β-CD is restricted. Using γ-CD, we obtained a tri-exponential function, having times of ~100 ps (82%), ~650 ps (9%) and ~ 4.23 ns (9%) assigned to free K* in water and to encapsulated K* and KR*, respectively. Gating at 560 nm (red side), the contribution of the ns-component due to caged KR* increases to 14%. It is worth to note that the protection of the guest by both cavities leads to longer lifetimes of K* and KR*, providing evidence that the confinement governs the relaxation route of the formed tautomers. In the case of HAN:α-CD the situation is different because of the existence of 1:1 and 1:2 complexes. The obtained lifetimes from the analysis of the emission decay of HAN in saturated solution of α-CD are ~90 ps (29%), ~1.0 ns (70%) and 5.1 ns (0.5%). We observed a considerable variation in the amplitude of ~1 ns component (from 2% to 70% when the [α-CD] changes from 3 to 110 mM). Therefore, we assigned this component to 1:2 complexes where the formation of KR* tautomer is not favourable due to the restrictions of the cavity. For 1:1 complex the lifetime is ~90 ps, similar to that in water. In a smaller cavity (α-CD), the $COHCH_3$ group of the guest is found outside of the cage, and therefore K* structure should not suffer any confinement effect.

For time-resolved anisotropy experiments, in pure water and THF (similar to CD from the point of view of polarity), the rotational times (ϕ) are ~70 and ~35 ps, respectively. This reflects the H-bonding effect on the friction dynamics of HAN. For β-CD solutions, the fit of the anisotropy decay gives two rotational times: $\phi_1 = \sim 70$ ps (45%) and $\phi_2 = \sim 745$ ps (55%). However, for γ-CD solutions we got $\phi_1 = \sim 47$ ps (54%) and $\phi_2 = \sim 1.1$ ns (46%). ϕ_1 was assigned to free tautomer rotational time, while ϕ_2 depends on the complexes and cavity sizes. For α-CD, the situation is different: ϕ_1 varies from 50 to 180 ps when we gated the anisotropy from 480 to 560 nm, while $\phi_2 = 950$ ps remains unchanged. The variation in ϕ_1 suggests the existence of several rotors that emit at different regions of the spectrum, while ϕ_2 reflects the overall rotational time of 1:2 complexes.

Conclusion

The present work shows different effects of CD confinement on the photophysical behaviours of the studied molecules.

For ADMB, an analogous to procaine and tetracaine, the emission lifetimes and quantum yield show a large increase upon CD encapsulation. The observation of two lifetimes for the complexes is explained in terms of different heterogeneous environments at the gate of CD leading to different interactions of water molecules with the amino and ester groups. In addition to the confinement of CD, these results are explained in terms of the interaction of the guest with water molecules located at both gates of CD.

For 3-HF, the cooperative H-bonding network of CD is important in the deprotonation and stabilization of 3HF. This leads to a caged anionic structure. The formation of a caged zwitterionic structure is not favourable due to the breaking of the intramolecular H-bond into the CD. The lifetime of the caged anion is in the ns regime.

For HAN, the twisting motion in the excited and caged tautomer K*, which will lead to KR*, might be controlled by the size of the cavity of CD. The spectroscopy and dynamic of the caged HAN depends on the nature of CD, where the confinement plays a key role.

We believe that the results of studying the selected three systems in this work might be of great interest for a

better understanding of CD complexes chemistry and its photodynamics.

Acknowledgments

This work was supported by the MEC and the JCCM through the projects: MAT2002-01829, SAN-04-000-00 and PBI-05-046.

References

1. A. Douhal: *Chem. Rev*. **104**, 1955 (2004).
2. Special Issue of *J. Photochem. Photobiol. A: Chem.* **173**, 229 (2005).
3. N. Nandi, K. Bhattacharyya, and B. Bagchi: *Chem. Rev*. **100**, 2013 (2000).
4. S.K. Mondal, K. Sahu, P. Sen, D. Roy, S. Ghosh, and K. Bhattacharyya: *Chem. Phys. Lett*. **412**, 228 (2005).
5. N. Sarkar, K. Das, D. Nath, and K. Bhattacharyya: *Chem. Phys. Lett*. **196**, 491 (1992).
6. D.P. Zhong, A. Douhal, and A.H. Zewail: *Proc. Natl. Acad. Sci. USA* **97**, 14052 (2000).
7. A. Douhal, T. Fiebig, M. Chachisvilis, and A.H. Zewail: *J. Phys Chem. A* **102**, 1657 (1998).
8. M. Chachisvilis, I. Garcia-Ochoa, A. Douhal, and A.H. Zewail: *Chem. Phys. Lett*. **293**, 153 (1998).
9. I. García-Ochoa, M.-A. Díez López, M.H. Viñas, L. Santos, E. Martínez Ataz, F. Sánchez, and A. Douhal: *Chem. Phys. Lett*. **296**, 335 (1998).
10. J.A. Organero, L. Tormo, and A. Douhal: *Chem. Phys. Lett*. **363**, 409 (2002).
11. J.A. Organero and A. Douhal: *Chem. Phys. Lett*. **373**, 426 (2003).
12. L. Tormo and A. Douhal: *J. Photochem. Photobiol. A Chem*. **173**, 358 (2005).
13. L. Tormo, J.A. Organero, and A. Douhal: *J. Phys. Chem. B* **109**, 17848 (2005).
14. T.A. Fayed, J.A. Organero, I. Garcia-Ochoa, L. Tormo, and A. Douhal: *Chem. Phys. Lett*. **364**, 108 (2002).
15. L. Tormo, J. A. Organero, and A. Douhal: In A. Douhal and J. Santamaria, (eds.) *Femtochemistry and Femtobiology: Ultrafast Dynamics in Molecular Science*, World Scientific, Singapore (2002), pp. 824–828.
16. A.J.G. Strandjord and P.F. Barbara: *J. Phys. Chem*. **89**, 2355 (1985).
17. M. Itoh and H. Kurokawa: *Chem. Phys. Lett*. **91**, 487 (1982).
18. S.J. Formosinho and L.G. Arnaut: *J. Photochem. Photobiol. A Chem* **75**, 21 (1993).
19. S.M. Dennison, J. Guharay, and P.K. Sengupta: *Spectrochim. Acta A* **55**, 903 (1999).
20. M. Itoh, K. Tokumura, Y. Tanimoto, Y. Okada, H. Takeuchi, K. Obi, and I. Tanaka: *J. Am. Chem. Soc*. **104**, 4146 (1982).
21. A.J.G. Strandjord, S.H. Courtney, D.M. Friedrich, and P.F. Barbara: *J. Phys. Chem*. **87**, 1125 (1983).
22. P.T. Dzygan, J. Schmidt, and T.J. Artsma: *Chem. Phys. Lett*. **127**, 336 (1986).
23. A. Douhal, M. Sanz, L. Tormo, and J.A. Organero: *Chem. Phys. Chem* **6**, 419 (2005).
24. S. Lochbrunner, T. Schultz, J.P. Shaffer, M.Z. Zgierski, and A. Stolow: *J. Chem. Phys*. **114**, 2519 (2001).
25. A. Douhal, F. Lahmani, and A. Zehnacker-Rentien: *Chem. Phys* **178**, 493 (1993).
26. A. Douhal, F. Lahmani, and A.H. Zewail: *Chem. Phys*. **207**, 477 (1996).
27. S. Tobita, M. Yamamoto, N. Kurahayashi, R. Tsukagoshi, Y. Nakamura, and H. Shizuka: *J. Phys. Chem. A* **102**, 5206 (1998).
28. C. Lu, R.-M.-R. Hsieh, I.-R. Lee, and P.-Y. Cheng: *Chem. Phys. Lett*. **310**, 102 (1999).
29. D.A. Southern, D.H. Levy, G.M. Florio, A. Longarte, and T.S. Zwier: *J. Phys. Chem. A* **107**, 4032 (2003).
30. A.L. Sobolewski and W. Domcke: *J. Phys. Chem. A* **108**, 10917 (2004).